Chapter 10
Development of a Method for Determining One of the Additional Elastic Moduli of Curvilinear Rods

Elena A. Ivanova and Valentina A. Timoshenko

Abstract In this paper we suggest a method for determining one of the additional elastic moduli in curvilinear rod theory. The method is based on the comparison of the analytical solution of the problem of static curvilinear rod bending with the numerical solution of the corresponding 3D problem. The method can be used for rods with any section shape and any microstructure.

Key words: Curvilinear rods · Thin-walled structures · Elastic moduli · Numerical experiment

10.1 Introduction

The rod model has been known for a long time and is widely used in engeneering analysis. However, there are still a lot of unsolved problems in the rod theory. An overview of investigations in modern rod theory can be found in Ghuku and Saha (2017). The research of statics, dynamics and stability of curvilinear rods is one of the most significant research directions (Ghuku and Saha, 2016; Satō, 1959; Tarn and Tseng, 2012; Sugiyama et al, 2006; Shiva Shankar and Vijayarangan, 2006; Gummadi and Palazotto, 1998; Erkmen and Bradford, 2009; Pippard, 1990; François et al, 2010). It is well known that two approaches are used for the formulation of

Elena A. Ivanova
Higher School of Theoretical Mechanics, Peter the Great St.Petersburg Polytechnic University, Polytechnicheskaya, 29, 195251, Saint-Petersburg & Institute for Problems in Mechanical Engineering of Russian Academy of Sciences, Bolshoy pr. V.O., 61, 199178, Saint-Petersburg, Russia
e-mail: elenaivanova239@gmail.com

Valentina A. Timoshenko
Higher School of Theoretical Mechanics, Peter the Great St.Petersburg Polytechnic University, Polytechnicheskaya, 29, 195251, Saint-Petersburg, Russia
e-mail: alya.tim.2012@mail.ru

H. Altenbach et al. (eds.), *Analysis of Shells, Plates, and Beams*, Advanced Structured Materials 134,
https://doi.org/10.1007/978-3-030-47491-1_10

the rod theory equations. They are the asymptotic one Berdichevskii (1981); Rubin (2000); Tiba and Vodak (2005); Meunier (2008); Jurak and Tambača (2001) and the direct one Svetlitsky (2000, 2005); Zhilin (2006, 2007); Altenbach et al (2006, 2012, 2013). If we consider the asymptotic approach, the formulae for the elastic moduli are obtained during the formulation of the basic equations, and this is an advantage of the approach. On the other hand, it is evident that if the rod has a complex configuration or complex internal structure, the use of mentioned approach becomes quite problematic. For the direct approach, the complexity of the configuration and internal structure do not influence the formulation of the basic equations, but in this case the determination of the elastic moduli becomes the separate research. A method for determining the elastic moduli and in the simpliest cases the elastic moduli themselves are well known for straight rods. The situation is completely different with curvilinear rods. In addition to those elastic moduli that straight rods have, there are several additional elastic moduli in curvilinear rod theory Zhilin (2006, 2007); Altenbach et al (2006, 2012, 2013). The additional moduli can be neglected if the rod is thin enough. But the additional elastic moduli can be important in the case of thick rods. Consequently, the development of a method for their determination is an important problem. In this paper we suggest the method for determining one of the additional elastic moduli of curvilinear rods.

10.2 Basic Equations of the Linear Theory of Curvilinear Rods

In this section we consider the basic equations of the linear theory of curvilinear rods, which has been suggested in Zhilin (2006, 2007) and further developed in Altenbach et al (2006, 2012, 2013). The model of the curvilinear rod is the directed curve. Reference configuration is defined by the position vector $\mathbf{r}(s)$, where s is the coordinate along the curve. Further we consider two triples: natural triple $\mathbf{t}$, $\mathbf{n}$, $\mathbf{b}$ and additional triple $\mathbf{d}_1$, $\mathbf{d}_2$, $\mathbf{d}_3$. Vectors $\mathbf{t}$, $\mathbf{n}$ and $\mathbf{b}$ are the unit vectors of tangent, normal and binormal respectively. The triple of mutually perpendicular unit vectors $\mathbf{d}_1$, $\mathbf{d}_2$, $\mathbf{d}_3$ associated with the cross-section of the rod. Vector $\mathbf{d}_3$ coincides with the direction of targent vector $\mathbf{t}$, and vectors $\mathbf{d}_1$, $\mathbf{d}_2$ are placed in the cross-section plane (see Fig. 10.1).

In the linear theory the motion equations are

$$\mathbf{T}' + \rho_0 \mathbf{f} = \rho_0 \dot{\mathcal{K}}_1, \quad \mathbf{M}' + \mathbf{t} \times \mathbf{T} + \rho_0 \mathbf{m} = \rho_0 \dot{\mathcal{K}}_2. \tag{10.1}$$

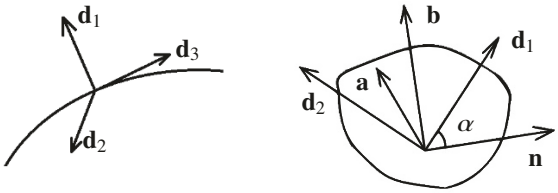

Fig. 10.1 The directed curve and position of the triple vectors in the cross-section

Here the prime represents the derivative with respect to the spatial coordinate, the dot represents the time derivative, **T** and **M** are the force and the moment in the cross-section, ρ_0 is the linear density of mass in the reference configuration, **f** and **m** are the external force and the external moment per unit mass, $\mathcal{K}_1$ and $\mathcal{K}_2$ are the linear momentum vector and the angular momentum vector per unit mass.

The kinetic energy per unit mass is

$$\mathcal{K} = \frac{1}{2}\mathbf{v}\cdot\mathbf{v} + \mathbf{v}\cdot\boldsymbol{\Theta}_1\cdot\boldsymbol{\omega} + \frac{1}{2}\boldsymbol{\omega}\cdot\boldsymbol{\Theta}_2\cdot\boldsymbol{\omega}, \tag{10.2}$$

where **v** is the velocity vector, $\boldsymbol{\omega}$ is the angular velocity vector, $\boldsymbol{\Theta}_1$ and $\boldsymbol{\Theta}_2$ are the inertia tensors per unit mass. The tensors $\boldsymbol{\Theta}_1$ and $\boldsymbol{\Theta}_2$ are time independent in the linear theory, but can be dependent on the spartial coordinate. The linear momentum vector and the angular momentum vector per unit mass are defined as partial derivatives of the kinetic energy per unit mass with respect to the velocity and angular velocity vectors respectively:

$$\mathcal{K}_1 = \frac{\partial\mathcal{K}}{\partial\mathbf{v}} = \mathbf{v} + \boldsymbol{\Theta}_1\cdot\boldsymbol{\omega}, \qquad \mathcal{K}_2 = \frac{\partial\mathcal{K}}{\partial\boldsymbol{\omega}} = \mathbf{v}\cdot\boldsymbol{\Theta}_1 + \boldsymbol{\Theta}_2\cdot\boldsymbol{\omega}. \tag{10.3}$$

The linear density of mass ρ_0 and the inertia tensors per unit length $\rho_0\boldsymbol{\Theta}_1$, $\rho_0\boldsymbol{\Theta}_2$ are

$$\rho_0 = \int\limits_{(\mathcal{F})} \rho^{(3)}\mu\,\mathrm{d}\mathcal{F}, \quad \rho_0\boldsymbol{\Theta}_1 = -\mathbf{E}\times\int\limits_{(\mathcal{F})} \rho^{(3)}\mathbf{a}\,\mu\,\mathrm{d}\mathcal{F}, \quad \rho_0\boldsymbol{\Theta}_2 = \int\limits_{(\mathcal{F})} \rho^{(3)}\big(\mathbf{a}\cdot\mathbf{a}\,\mathbf{E} - \mathbf{aa}\big)\mu\,\mathrm{d}\mathcal{F}, \tag{10.4}$$

with

$$\mu = 1 + \frac{1}{R_c}\mathbf{n}\cdot\mathbf{a}.$$

Here $\rho^{(3)}$ is the mass density per unit volume, $\mathcal{F}$ is a cross-section area, **E** is the unit tensor, R_c is the radius of curvature, **a** is a vector, which connects the centre and some point of the cross-section (see Fig. 10.1).

The internal energy is the quadratic form of the deformation vectors in the linear theory:

$$\rho_0\mathcal{U} = \frac{1}{2}\boldsymbol{\mathcal{E}}\cdot\mathbf{A}\cdot\boldsymbol{\mathcal{E}} + \boldsymbol{\mathcal{E}}\cdot\mathbf{B}\cdot\boldsymbol{\Phi} + \frac{1}{2}\boldsymbol{\Phi}\cdot\mathbf{C}\cdot\boldsymbol{\Phi}. \tag{10.5}$$

Here $\mathcal{U}$ is the internal energy per unit mass, $\boldsymbol{\mathcal{E}}$ is the vector of extension-shear deformation, $\boldsymbol{\Phi}$ is the vector of bending-twisting deformation, **A**, **B**, **C** are the elasticity tensors. Tensor **A** is responsible for extension and transverse shear, tensor **C** is responsible for bending and twisting, tensor **B** characterizes the mutual influence of the extension-shear deformations and the bending-twisting deformations. If we consider the straight rod and the natural twisting is absent, the tensor **B** is equal to zero. The tensors **A**, **B**, **C** are time independent in the linear theory, but can be dependent on spartial coordinate. The deformation vectors are

$$\boldsymbol{\mathcal{E}} = \mathbf{u}' + \mathbf{t}\times\boldsymbol{\psi}, \qquad \boldsymbol{\Phi} = \boldsymbol{\psi}', \tag{10.6}$$

where $\mathbf{u}$ is the displacement vector, $\boldsymbol{\psi}$ is the rotation vector. The constitutive equations have the form

$$\mathbf{T} = \frac{\partial(\rho_0 \mathcal{U})}{\partial \boldsymbol{\mathcal{E}}} = \mathbf{A} \cdot \boldsymbol{\mathcal{E}} + \mathbf{B} \cdot \boldsymbol{\Phi}, \qquad \mathbf{M} = \frac{\partial(\rho_0 \mathcal{U})}{\partial \boldsymbol{\Phi}} = \boldsymbol{\mathcal{E}} \cdot \mathbf{B} + \mathbf{C} \cdot \boldsymbol{\Phi}. \tag{10.7}$$

The elasticity tensors have the following structure for curvilinear rods without the natural twisting:

$$\begin{aligned}
\mathbf{A} &= A_1 \mathbf{d}_1 \mathbf{d}_1 + A_2 \mathbf{d}_2 \mathbf{d}_2 + A_3 \mathbf{d}_3 \mathbf{d}_3, \\
\mathbf{C} &= C_1 \mathbf{d}_1 \mathbf{d}_1 + C_2 \mathbf{d}_2 \mathbf{d}_2 + C_3 \mathbf{d}_3 \mathbf{d}_3, \\
\mathbf{B} &= \frac{1}{R_c}\Big[(B_{23}\mathbf{d}_2\mathbf{d}_3 + B_{32}\mathbf{d}_3\mathbf{d}_2)\cos\alpha + (B_{13}\mathbf{d}_1\mathbf{d}_3 + B_{31}\mathbf{d}_3\mathbf{d}_1)\sin\alpha\Big] \\
&\quad + \frac{1}{R_t}(B_1 \mathbf{d}_1 \mathbf{d}_1 + B_2 \mathbf{d}_2 \mathbf{d}_2 + B_3 \mathbf{d}_3 \mathbf{d}_3),
\end{aligned} \tag{10.8}$$

where R_t is the radius of torsion, α is an angle between the vectors $\mathbf{d}_1$, $\mathbf{d}_2$ and the vectors $\mathbf{n}$, $\mathbf{b}$ (see Fig. 10.1). Other scalar coefficients in Eq. (10.8) represent the elastic moduli. The elastic moduli A_k and C_k are determined during the experiments with straight rods. The elastic moduli B_{ij} can be determined during the experiments with plane curvilinear rods. The elastic moduli B_k can be determined during the experiments with spatially curved rods.

We need formulae relating the characteristics of stress-strain state of the rod and the three-dimensional body for interpretation of the data from physical and numerical experiments. In the linear theory the force and moment vectors in the cross-section of the rod are the integral characteristics of stress in cross-section of the three-dimensional body. The corresponding formulae are generally accepted. Different authors determine the relationships between the kinematic characteristics differently. In considered theory for comparison of the kinematic characteristics we use the assumption that the linear momentum vector and the angular momentum vector of the rod and the three-dimensional body must be the same. The mentioned relationships are easily integrated over time, as a result we get the relationship between the displacement vector, the rotation vector and the integral characteristics of the displacement vector of three-dimensional body. This way we get the following relationships:

$$\begin{aligned}
&\mathbf{T} = \int\limits_{(\mathcal{F})} \mathbf{t} \cdot \boldsymbol{\tau}\, \mathrm{d}\mathcal{F}, \qquad \mathbf{M} = \int\limits_{(\mathcal{F})} \mathbf{a} \times (\mathbf{t} \cdot \boldsymbol{\tau})\, \mathrm{d}\mathcal{F}, \\
&\rho_0 (\mathbf{u} + \boldsymbol{\Theta}_1 \cdot \boldsymbol{\psi}) = \int\limits_{(\mathcal{F})} \rho^{(3)} \mathbf{u}^{(3)}\, \mu\, \mathrm{d}\mathcal{F}, \\
&\rho_0 (\mathbf{u} \cdot \boldsymbol{\Theta}_1 + \boldsymbol{\Theta}_2 \cdot \boldsymbol{\psi}) = \int\limits_{(\mathcal{F})} \rho^{(3)} \mathbf{a} \times \mathbf{u}^{(3)}\, \mu\, \mathrm{d}\mathcal{F}.
\end{aligned} \tag{10.9}$$

Here $\boldsymbol{\tau}$ is the stress tensor, $\mathbf{u}^{(3)}$ is the displacement vector in the 3D-theory. Eq. (10.9) form the method of the numerical experiment.

10.3 Formulation and Solution of the Model Problem

The aim of this research is to formulate the model problem, which solution provides the opportunity of determination of the elastic modulus B_{32}. In this section we discuss the formulation and numerical solution of the model problem within the rod theory, the formulation of the corresponding problem within the 3D-theory and the relationships that allow us to compare the solutions of mentioned problems.

We consider the plane curvilinear rod, which has a form of $3/4$ of the circle with the radius R. We also assume that the principal axes of inertia of the cross-section coincide with the vectors of the natural triple. This way $\alpha = 0$, $R_t = \infty$. It is obviously that the use of cylindrical coordinate system r, θ, z (see Fig. 10.2) is convenient for the model problem. The following relationships occur:

$$s = r\theta, \quad \mathbf{d}_1 = \mathbf{n} = -\mathbf{e}_r, \quad \mathbf{d}_2 = \mathbf{b} = \mathbf{k}, \quad \mathbf{d}_3 = \mathbf{t} = \mathbf{e}_\theta, \quad R_c = -R. \tag{10.10}$$

We consider the static deformation of the rod. One end of the rod is rigidly fixed and another end is loaded only by the moment, which deforms the rod without taking it out the plane. External forces and moments distributed along the length of the rod are absent. In the rod theory we formulate this problem as

$$\begin{aligned} &\mathbf{T}' = 0, \quad \mathbf{M}' + \mathbf{t}\times\mathbf{T} = 0, \quad \boldsymbol{\mathcal{E}} = \mathbf{u}' + \mathbf{t}\times\boldsymbol{\psi}, \qquad \boldsymbol{\Phi} = \boldsymbol{\psi}', \\ &\mathbf{T} = \mathbf{A}\cdot\boldsymbol{\mathcal{E}} + \mathbf{B}\cdot\boldsymbol{\Phi}, \quad \mathbf{M} = \boldsymbol{\mathcal{E}}\cdot\mathbf{B} + \mathbf{C}\cdot\boldsymbol{\Phi}, \\ &\mathbf{u}|_{s=0} = 0, \quad \boldsymbol{\psi}|_{s=0} = 0, \quad \mathbf{T}|_{s=0} = 0, \quad \mathbf{M}|_{s=l} = M_0\mathbf{k}, \end{aligned} \tag{10.11}$$

where M_0 is the external moment. Taking into account the structure of the tensors from Eq. (10.8), we obtain the solution of Eq. (10.11):

$$\mathbf{u} = u_n\mathbf{n} + u_t\mathbf{t}, \qquad \boldsymbol{\psi} = \psi_b\mathbf{b}, \tag{10.12}$$

where

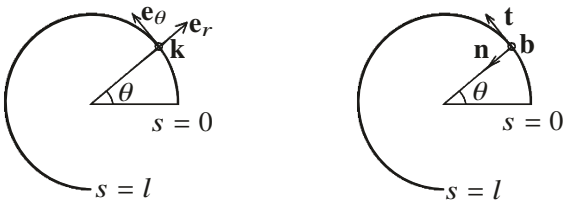

Fig. 10.2 The natural triple and the cylindrical coordinate system

$$u_n = M_0 R^2 \left(C_2 - \frac{B_{32}^2}{R^2 A_3} \right)^{-1} \left(1 - \frac{B_{32}}{R^2 A_3} \right) \left(1 - \cos \frac{s}{R} \right),$$
$$u_t = M_0 R^2 \left(C_2 - \frac{B_{32}^2}{R^2 A_3} \right)^{-1} \left(\frac{s}{R} - \left(1 - \frac{B_{32}}{R^2 A_3} \right) \sin \frac{s}{R} \right), \qquad (10.13)$$
$$\psi_b = M_0 s \left(C_2 - \frac{B_{32}^2}{R^2 A_3} \right)^{-1}.$$

From Eqs. (10.12), (10.13), it follows that the rod is deformed in the plane and the solution depends on three elastic moduli. These moduli are the extension elastic modulus A_3, the bending elastic modulus C_2 and the additional elastic modulus B_{32}. It is important that the solution of the model problem depends on only one unknown elactic modudus. If the elastic modulus $B_{32} = 0$, Eq. (10.13) simplifies and has the form

$$u_n^c = \frac{M_0 R^2}{C_2} \left(1 - \cos \frac{s}{R} \right),$$
$$u_t^c = \frac{M_0 R^2}{C_2} \left(\frac{s}{R} - \sin \frac{s}{R} \right), \qquad (10.14)$$
$$\psi_b^c = \frac{M_0 s}{C_2}.$$

Comparison of the solutions of Eqs. (10.13) and (10.14) shows that the elastic modulus B_{32} has an effect on the solution of the problem and also provides the effect of the elastic modulus A_3.

Figure 10.3 illustrates the formulation of the corresponding problem in 3D-theory. We consider the body, which is $3/4$ of the hollow cylinder. The height of the cylinder is b, the difference between the internal and external raduii is a, the radius of the midline, i.e. the line passing through the centres of the sections, is equal to the radius R of the rod. The surface of the cylinder $\theta = 0$ is rigidly fixed. There is a distributed load on the surface $\theta = 3\pi/2$, which causes the resultant force equal to zero and the resultant moment M_0. The other cylinder surfaces are free. As a result

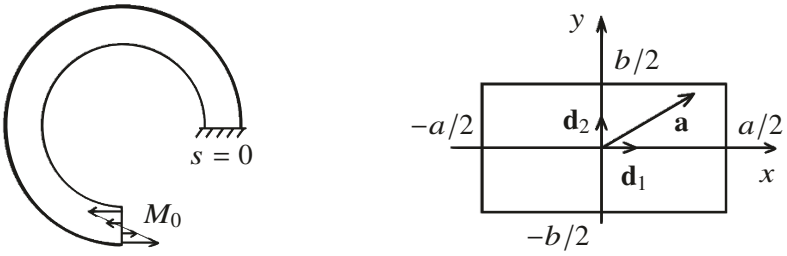

Fig. 10.3. Boundary conditions and the local coordinate system in the cross-section

of numerical solution we determine the displacement field $\mathbf{u}^{(3)}$ in the cylindrical coordinate system:

$$\mathbf{u}^{(3)} = u_r^{(3)}\mathbf{e}_r + u_\theta^{(3)}\mathbf{e}_\theta + u_z^{(3)}\mathbf{k}. \tag{10.15}$$

Taking into account Eqs. (10.4), (10.9) and writing vector $\mathbf{a}$ (see Fig. 10.3) as

$$\mathbf{a} = x\mathbf{d}_1 + y\mathbf{d}_2, \tag{10.16}$$

we get the following integral relationships between the components of the displacement and rotation vectors in the rod theory and the components of the displacement vector in the 3D-theory

$$\begin{aligned}
u_n &= -\frac{1}{ab}\int\limits_{-\frac{a}{2}}^{\frac{a}{2}}\int\limits_{-\frac{b}{2}}^{\frac{b}{2}} u_r^{(3)}\left(1-\frac{x}{R}\right)\mathrm{d}x\mathrm{d}y,\\
u_t &= \frac{1}{ab}\left(1-\frac{a^2}{12R^2}\right)^{-1}\int\limits_{-\frac{a}{2}}^{\frac{a}{2}}\int\limits_{-\frac{b}{2}}^{\frac{b}{2}} u_\theta^{(3)}\left(1-\frac{x^2}{R^2}\right)\mathrm{d}x\mathrm{d}y,\\
\psi_b &= -\frac{1}{abR}\left(1-\frac{a^2}{12R^2}\right)^{-1}\int\limits_{-\frac{a}{2}}^{\frac{a}{2}}\int\limits_{-\frac{b}{2}}^{\frac{b}{2}} u_\theta^{(3)}\left(1+\frac{12Rx}{a^2}\right)\left(1-\frac{x}{R}\right)\mathrm{d}x\mathrm{d}y.
\end{aligned} \tag{10.17}$$

Thus, if we get the numerical solution of the 3D-problem, we can calculate components u_n, u_t and ψ_b in current cross-section of the rod using Eq. (10.17). After their substitution into Eq. (10.13), we get three expessions for determining the elastic modulus B_{32}. From the theoretical point of view the value of the modulus B_{32} should be independent of the choice of the expression. This value also should be independent of the cross-section position. However, the elastic modulus B_{32} depends on the position of the cross-section and the chosen equation in fact. It is the reason why the choice of the method for determining the elastic modulus B_{32} is very important. We choose the method with respect to the less dependency on the cross-section position.

10.4 Method for Determining the Elastic Modulus B_{32}

In this section we consider three methods for determining the elastic modulus B_{32}. For better presentation of the difference between the methods for determining the elastic modulus we perform the calculations for the body, which is not very similar to the rod. This body has the radius of the midline $R = 0{,}5$ m, its cross-section is the square with the sides length $a = b = 0{,}2$ m. We choose the steel with Young's

modulus $E = 2 \cdot 10^{11}$ N/m^2 and Poisson's ratio $\nu = 0.33$ as a material. For the chosen body:

$$A_3 = Ea^2 = 8 \cdot 10^9 \text{ N}, \quad A_3 R^2 = 2 \cdot 10^9 \text{ Nm}^2, \quad C_2 = \frac{Ea^2}{12} = 2.67 \cdot 10^7 \text{ N}. \quad (10.18)$$

In this section and further all values of the elastic moduli are in the SI. The external moment equals $M_0 = 150000$ N·m. The calculations are done with a software application ABAQUS. We use cubic finite element with the side length 0,005 m. The investigation of the convergence shows that the numerical solution converges even for coarse mesh. Decrease of the mesh element length increases the accuracy of the calculations of the integrals from Eq. (10.17). We use the displacements and rotation angles from Eq. (10.17) in three cross-sections $\theta = 3\pi/4$, $\theta = \pi$, $\theta = 5\pi/4$ (it also is necessary to consider the cross-section $\theta = \pi/2$ for one calculation series) for determining the elastic modulus B_{32}. The choice of the cross-sections is explained by the fact that their positions are quite far from each other and the boundaries (see Fig. 10.4).

- ***The first method*** uses the coefficient

$$\left(C_2 - \frac{B_{32}^2}{R^2 A_3}\right)^{-1} \left(1 - \frac{B_{32}}{R^2 A_3}\right).$$

According to Eq. (10.13), there are two ways to calculate the mentioned coefficient. The first one uses the value of the component u_n in the cross-section s_* as

$$\left(C_2 - \frac{B_{32}^2}{R^2 A_3}\right)^{-1} \left(1 - \frac{B_{32}}{R^2 A_3}\right) = \frac{u_n(s_*)}{M_0 R^2 (1 - \cos(s_*/R))} \quad (10.19)$$

and the second one uses the value of the difference $u_t - R\psi_b$ in the cross-section s_* as

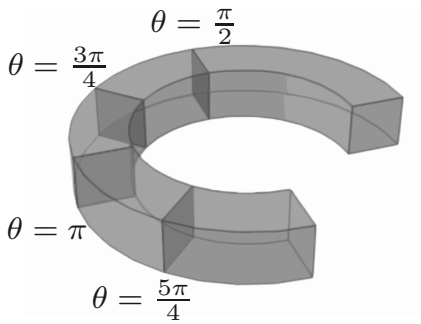

Fig. 10.4 The position and angles of chosen cross-sections

$$\left(C_2 - \frac{B_{32}^2}{R^2 A_3}\right)^{-1} \left(1 - \frac{B_{32}}{R^2 A_3}\right) = \frac{R\psi_b(s_*) - u_t(s_*)}{M_0 R^2 \sin(s_*/R)}. \tag{10.20}$$

The calculation results are presented in Table 10.1. Obviously we cannot calculate the coefficient using the values $u_t - R\psi_b$, but the way of calculation using the values of the component u_n is highly accurate. However, solving Eq. (10.19) we obtain complex values of the modulus B_{32}, the imaginary parts of which are comparable to the real parts. It means that this method of determining the elastic modulus B_{32} is unacceptable.

- ***The second method*** supposes the use of the coefficient

$$\left(C_2 - \frac{B_{32}^2}{R^2 A_3}\right)^{-1}.$$

According to Eq. (10.13), this coefficient can be calculated in three ways. The first one uses the value of the component ψ_b in the cross-section s_* as

$$\left(C_2 - \frac{B_{32}^2}{R^2 A_3}\right)^{-1} = \frac{\psi_b(s_*)}{M_0 R s_*}, \tag{10.21}$$

the second one uses the value of the component u_t in the cross-section with $s_* = \pi R$ as

$$\left(C_2 - \frac{B_{32}^2}{R^2 A_3}\right)^{-1} = \frac{u_t(s_*)}{M_0 R^2 s_*}, \tag{10.22}$$

and the third one uses the value of the sum $u_n + u_t$ in the cross-section $s_* = \pi R/2$, i.e. the cross-section, where

$$1 - \cos\frac{s}{R} = \sin\frac{s}{R},$$

as

Table 10.1

Coefficient values $\left(C_2 - \frac{B_{32}^2}{R^2 A_3}\right)^{-1} \left(1 - \frac{B_{32}}{R^2 A_3}\right)$

Cross-section	Using u_n	Error, using u_n	Using $u_t - R\psi_b$	Error, using $u_t - R\psi_b$
$3\pi/4$	$3,67 \cdot 10^{-8}$	0,90 %	$4,8 \cdot 10^{-8}$	52,84 %
π	$3,65 \cdot 10^{-8}$	0,41 %	-	-
$5\pi/4$	$3,59 \cdot 10^{-8}$	1,31 %	$1,48 \cdot 10^{-8}$	52,84 %

$$\left(C_2 - \frac{B_{32}^2}{R^2 A_3}\right)^{-1} = \frac{u_n(s_*) + u_t(s_*)}{M_0 R s_*}. \tag{10.23}$$

The calculation results are presented in Table 10.2. It is evident that the way based on the use of the values of the component ψ_b is highly accurate. The value calculated using the sum $u_n + u_t$ corresponds the general tend to decreasing of the value as the cross-section gets closer to the fixed end. The coefficient value calculated using the component u_t is smaller than other values, and we suppose it to be questionable.

From the theoretical point of view the elastic modulus B_{32} can be positive or negative. It is clear that the suggested method allows us to determine the absolute value of modulus B_{32}. In Table 10.3 we present positive values of the modulus B_{32}. An analysis of the results shows that the method for determining the elastic modulus B_{32} using Eq. (10.21) allows us to obtain the values, which slightly depend on the choice of the cross-section. Thus this method is acceptable. It has the only disadvantage that we cannot determine the sign of the elastic modulus B_{32}.

- ***The third method*** uses the values of the coefficient

$$\left(1 - \frac{B_{32}}{R^2 A_3}\right).$$

According to Eq. (10.13), we can calculate this coefficient in three ways. The first one consists in the use of the ratio u_n/u_t in the cross-section s_* as

Table 10.2

Coefficient values $\left(C_2 - \frac{B_{32}^2}{R^2 A_3}\right)^{-1}$

Cross-section	Using $u_n + u_t$	Using u_t	Using ψ_b	Error, using ψ_b
$\pi/2$	$3,91 \cdot 10^{-8}$	-	-	-
$3\pi/4$	-	-	$4,08 \cdot 10^{-8}$	1,18 %
π	-	$3,76 \cdot 10^{-8}$	$4,14 \cdot 10^{-8}$	0,18 %
$5\pi/4$	-	-	$4,17 \cdot 10^{-8}$	1,00 %

Table 10.3

The elastic modulus B_{32} calculated using $\left(C_2 - \frac{B_{32}^2}{R^2 A_3}\right)^{-1}$

Cross-section	Using $u_n + u_t$	Using u_t	Using ψ_b	Error, using ψ_b
$\pi/2$	$4,67 \cdot 10^{7}$	-	-	-
$3\pi/4$	-	-	$6,56 \cdot 10^{7}$	5,99 %
π	-	$1,19 \cdot 10^{7}$	$7,05 \cdot 10^{7}$	1,04 %
$5\pi/4$	-	-	$7,32 \cdot 10^{7}$	4,95 %

$$1-\frac{B_{32}}{R^2A_3}=\frac{u_n(s_*)\,s_*}{R\big[u_t(s_*)(1-\cos(s_*/R))+u_n(s_*)\sin(s_*/R)\big]}, \tag{10.24}$$

the second one consists in the use of the ratio u_n/ψ_b in the cross-section s_* as

$$1-\frac{B_{32}}{R^2A_3}=\frac{u_n(s_*)\,s_*}{R^2\psi_b(s_*)\big[1-\cos(s_*/R)\big]} \tag{10.25}$$

and the third one consists in the use of the ratio u_t/ψ_b in the cross-section s_* as

$$1-\frac{B_{32}}{R^2A_3}=\frac{\big[R\psi_b(s_*)-u_t(s_*)\big]s_*}{R^2\psi_b(s_*)\sin(s_*/R)}. \tag{10.26}$$

The calculation results are presented in Table 10.4. It is evident that the way based on the use of the ratio u_t/ψ_b is unacceptable at all. Others demonstrate the same dependency of the cross-section choice, but give different average values of the coefficient.

The results of calculation of the elastic modulus are presented in Table 10.5. An analysis of the results shows the noticeable difference between the values of the modulus B_{32} calculated using the ratio u_n/u_t and the values calculated using the ratio u_n/ψ_b. The substitution of the average values into the coefficient

$$\left(C_2-\frac{B_{32}^2}{R^2A_3}\right)^{-1}$$

Table 10.4
Coefficient values $\left(1-\frac{B_{32}}{R^2A_3}\right)$

Cross-section	Using u_n/u_t	Error, using u_n/u_t	Using u_n/ψ_b	Error, using u_n/ψ_b	Using u_t/ψ_b
$3\pi/4$	0,981	1,54 %	0,899	2,02 %	1,18
π	0,970	0,47 %	0,883	0,21 %	-
$5\pi/4$	0,946	2,01 %	0,860	2,31 %	0,36

Table 10.5
The elastic modulus B_{32}, calculated using $\left(1-\frac{B_{32}}{R^2A_3}\right)$

Cross-section	Using u_n/u_t	Error, using u_n/u_t	Using u_n/ψ_b	Error, using u_n/ψ_b
$3\pi/4$	$3,85\cdot10^7$	43,6 %	$2,02\cdot10^8$	15,44 %
π	$5,91\cdot10^7$	13,4 %	$2,35\cdot10^8$	1,58 %
$5\pi/4$	$10,7\cdot10^7$	56,9 %	$2,79\cdot10^8$	17,02 %

shows that this expression is positive if the modulus B_{32} is calculated using the ratio u_n/u_t, and the expression is negative if we substitute the values calculated using the ratio u_n/ψ_b. Consequently, the way of determining the modulus B_{32} using the ratio u_n/ψ_b is unacceptable.

Thus the only method for determining the sign of the elastic modulus consists in determining this modulus using the ratio u_n/u_t. From Table. 10.5 we see that this way gives the values dependent on the cross-section choice. However, the average value $B_{32} = 6{,}82 \cdot 10^7$ is close to the average value $B_{32} = 6{,}98 \cdot 10^7$ which is calculated using the components ψ_b. The relative difference between them is equal to 2,32 %.

10.5 Discussion

As a result of our study we conclude that considered model problem can be used for determining the elastic modulus B_{32} by the numerical experiment. The best of considered methods for determining this modulus is the method which uses Eq. (10.21). We can also use the method based on Eq. (10.24) for additional verification and determining the sign of modulus B_{32}.

In Zhilin (2007) the author considers the method for determining the elastic modulus B_{32}, based on the solution of a problem of the deformation of a closed circular rod under the action of a uniformly distributed radial load. The balance equations have the form

$$\mathbf{T}' + f\mathbf{n} = 0, \qquad \mathbf{M}' + \mathbf{t} \times \mathbf{T} = 0. \tag{10.27}$$

Due to axial symmetry the solution has the following structure:

$$\begin{aligned} \mathbf{u} &= u_n \mathbf{n}, & \boldsymbol{\psi} &= 0, \\ \boldsymbol{\mathcal{E}} &= \mathcal{E}_t \mathbf{t}, & \boldsymbol{\Phi} &= 0, \\ \mathbf{T} &= A_3 \mathcal{E}_t \mathbf{t}, & \mathbf{M} &= \frac{B_{32}}{R_c} \mathcal{E}_t \mathbf{b}. \end{aligned} \tag{10.28}$$

This model problem is interesting with the fact that the corresponding 3D-problem allows to find the analytical solution in the case if the height of the cylinder is small enough to allow us to consider the stress-strain state to be plane. The conparison of the 1D-problem solution and the 3D-problem solution leads to the simple formula $B_{32} = C_2$.

The calculated above value of B_{32} coincides with $B_{32} = C_2$ in an order of magnitude. However, the calculated value is about 2,5 times higher. Taking into account the specifics of the model problem considered in Zhilin (2007) and the fact that three-dimensional body used in our study is not very similar to the rod, we can consider the coincidence of the results as quite good.

The developed method can be used for determining the elastic modulus B_{32} in the case of curvilinear rods, which have different shapes of the cross-section and the arbitrarily complex internal structure.

References

Altenbach H, Naumenko K, Zhilin PA (2006) A direct approach to the formulation of constitutive equations for rods and shells. In: Pietraszkiewicz W, Szymczak C (eds) Shell Structures: Theory and Applications, Taylor and Francis, London, pp 87–90

Altenbach H, Bîrsan M, Eremeyev V (2012) On a thermodynamic theory of rods with two temperature fields. Acta Mechanica 223:1583–1596

Altenbach H, Bîrsan M, Eremeyev V (2013) Cosserat-type rods. In: Altenbach H, Eremeyev V (eds) Generalized Continua – from the theory to Engineering Applications, Springer, Wien, CISM International Centre for Mechanical Sciences, vol 541, pp 179–248

Berdichevskii V (1981) On the energy of an elastic rod. Journal of Applied Mathematics and Mechanics 45(4):518 – 529

Erkmen RE, Bradford MA (2009) Nonlinear elastic analysis of composite beams curved in-plan. Engineering Structures 31(7):1613 – 1624

François MLM, Semin B, Auradou H (2010) Identification of the shape of curvilinear beams and fibers. In: Advances in Experimental Mechanics VII, Trans Tech Publications Ltd, Applied Mechanics and Materials, vol 24-25, pp 359–364

Ghuku S, Saha KN (2016) A theoretical and experimental study on geometric nonlinearity of initially curved cantilever beams. Engineering Science and Technology, an International Journal 19(1):135 – 146

Ghuku S, Saha KN (2017) A review on stress and deformation analysis of curved beams under large deflection. International Journal of Engineering and Technologies 11:13–39

Gummadi L, Palazotto A (1998) Large strain analysis of beams and arches undergoing large rotations. International Journal of Non-Linear Mechanics 33(4):615 – 645

Jurak M, Tambača J (2001) Linear curved rod model: General curve. Mathematical Models and Methods in Applied Sciences 11(7):1237–1252

Meunier N (2008) Recursive derivation of one-dimensional models from three-dimensional nonlinear elasticity. Mathematics and Mechanics of Solids 13(2):172–194

Pippard AB (1990) The elastic arch and its modes of instability. European Journal of Physics 11(6):359–365

Rubin MB (2000) Cosserat Theories: Shells, Rods, and Points. Kluwer Academic Publishers, Dordrecht

Satō K (1959) Large deflection of a circular cantilever beam with uniformly distributed load. Ingenieur-Archiv 27(3):195 – 200

Shiva Shankar GS, Vijayarangan S (2006) Mono composite leaf spring for light weight vehicle–design, end joint analysis and testing. Materials Science 12(3):220–225

Sugiyama H, Shabana AA, Omar MA, Loh WY (2006) Development of nonlinear elastic leaf spring model for multibody vehicle systems. Computer Methods in Applied Mechanics and Engineering 195(50):6925 – 6941

Svetlitsky VA (2000) Statics of Rods. Foundations of Engineering Mechanics, Springer, Berlin-Heidelberg

Svetlitsky VA (2005) Dynamics of Rods. Foundations of Engineering Mechanics, Springer, Berlin-Heidelberg

Tarn JQ, Tseng WD (2012) Exact analysis of curved beams and arches with arbitrary end conditions: A Hamiltonian state space approach. Journal of Elasticity 107(1):39–63

Tiba D, Vodak R (2005) A general asymptotic model for Lipschitzian curved rods. Advances in Mathematical Sciences and Applications 15:137–198

Zhilin PA (2006) Nonlinear theory of thin rods. In: Indeitsev DA, Ivanova EA, Krivtsov AM (eds) Advanced Problems in Mechanics, Instit. Problems Mech. Eng. R.A.S. Publ, St. Petersburg, vol 2, pp 227–249

Zhilin PA (2007) Applied Mechanics. Theory of Thin Elastic Rods (in Russ.). Politekhn. Univ. Publ., St. Petersburg